Characteristics of Thermalization of Boost-Invariant Plasma from Holography

Michal P. Heller*

Instituut voor Theoretische Fysica, Universiteit van Amsterdam, Science Park 904, 1090 GL Amsterdam, The Netherlands

Romuald A. Janik† and Przemysław Witaszczyk‡

Institute of Physics, Jagiellonian University, Reymonta 4, 30-059 Kraków, Poland

(Received 25 March 2011; revised manuscript received 8 March 2012; published 18 May 2012)

We report on the approach toward the hydrodynamic regime of boost-invariant $\mathcal{N} = 4$ super Yang-Mills plasma at strong coupling starting from various far-from-equilibrium states at $\tau = 0$. The results are obtained through a numerical solution of Einstein's equations for the dual geometries, as described in detail in the companion article [M. P. Heller, R. A. Janik, and P. Witaszczyk, arXiv:1203.0755]. Despite the very rich far-from-equilibrium evolution, we find surprising regularities in the form of clear correlations between initial entropy and total produced entropy, as well as between initial entropy and the temperature at thermalization, understood as the transition to a hydrodynamic description. For 29 different initial conditions that we consider, hydrodynamics turns out to be definitely applicable for proper times larger than 0.7 in units of inverse temperature at thermalization. We observe a sizable anisotropy in the energy-momentum tensor at thermalization, which is nevertheless entirely due to hydrodynamic effects. This suggests that effective thermalization in heavy-ion collisions may occur significantly earlier than true thermalization.

DOI: 10.1103/PhysRevLett.108.201602 PACS numbers: 11.25.Tq, 12.38.Mh

Introduction.—One of the outstanding problems of the dynamics of quark-gluon plasma is the understanding of the physics of thermalization. In relativistic heavy-ion collisions at RHIC and LHC the quantitative description of experimental data requires the applicability of hydrodynamics from a very early stage [1]. However, our insight into the nonequilibrium dynamics of quark-gluon plasma is very scarce. The above problem is often referred to as ''the early thermalization puzzle.'' This is, in fact, a misnomer as viscous hydrodynamics may turn out to be applicable when the pressures are still quite anisotropic, going against the commonly accepted paradigm that true thermalization is necessary. One of the main results of the present work is that for *a wide range* of initial conditions this is indeed the case. Subsequent isotropization toward true thermodynamic equilibrium occurs purely within the quantitatively well understood viscous hydrodynamics and is trivial in comparison.

The key physical question of interest is the time scale after which the viscous hydrodynamic description becomes valid. This has a further refinement as viscous hydrodynamics is really a gradient expansion with new transport coefficients appearing at each order. So it is very interesting to determine to what extent would *all-order* resummed hydrodynamics describe the plasma evolution and to what extent is one forced to incorporate genuine nonhydrodynamic degrees of freedom. Furthermore, the dynamics of plasma expansion will strongly depend on the initial state. It is very important to understand if there exists some simple physical characterization of the initial state determining the characteristics of the transition to hydrodynamics and subsequent evolution. Finally, it is interesting to understand the amount of entropy produced during different stages of the dynamics.

In this Letter, we will address the above questions for plasma configurations invariant under longitudinal boosts and with no dependence on transverse coordinates. This kinematical regime was first introduced by Bjorken [2] and roughly mimics an infinite energy collision of infinitely large nuclei.

Within QCD there are no techniques allowing us to address these issues from first principles. It is thus quite natural to consider the same questions in the context of strongly coupled plasma in the $\mathcal{N} = 4$ supersymmetric gauge theory for the description of which one can use the AdS/CFT correspondence [3]. There, the time dependence of plasma is translated into gravitational dynamics in 5 dimensions with a negative cosmological constant and appropriate boundary conditions. Using these methods, perfect fluid hydrodynamics was derived at the nonlinear level in the boost-invariant setting [4], the value of shear viscosity was shown to agree [5] with the one extracted from linear perturbations [6], and finally, viscous hydrodynamics was derived without any symmetry assumptions [7].

Once we consider the far-from-equilibrium regime for small proper times, gradient or scaling expansions cease to be valid, and one has to deal with full Einstein's equations. Previous work by some of us [8], motivated by the early results of [9], used power series expansions around $\tau = 0$ to study the strongly nonequilibrium regime of Bjorken flow. Unfortunately, the radius of convergence of these power series was insufficient to analyze the transition to

hydrodynamics. On the other hand, the numerical work of [10] necessarily introduced a deformation of the physical 4-dimensional metric to pump energy and momentum into the vacuum at early times and create, in this way, a far-from-equilibrium state. Such a way of generating the initial state precludes the analysis of the physical evolution starting from $\tau = 0$, in particular, the investigation of the influence of the initial conditions on thermalization and entropy production that we are interested in.

Motivated by this, we developed a new numerical framework using the Arnowitt-Deser-Misner formalism of numerical relativity and analyzed the evolution of the plasma system starting from a range of initial conditions. These correspond, in our setup, to specifying a single metric coefficient function (*initial profile*) for the initial geometry on the hypersurface $\tau = 0$. The initial hypersurface is the same as in [8], however, without any spurious coordinate singularities. Subsequently we solve numerically 5-dimensional Einstein's equations and obtain the plasma energy-momentum tensor from the asymptotics of the solution at the anti–de Sitter boundary. The details of this setup can be found in a companion article [11], while in the present Letter we will concentrate on the physical questions mentioned above.

Boost-invariant plasma and hydrodynamics.—The traceless and conserved energy-momentum tensor of a boost-invariant conformal plasma system with no transverse coordinate dependence is uniquely determined in terms of a single function $\langle T_{\tau\tau}\rangle$—the energy density at midrapidity $\varepsilon(\tau)$. The longitudinal and transverse pressure are consequently given by

$$p_L = -\varepsilon - \tau\frac{d}{d\tau}\varepsilon \quad \text{and} \quad p_T = \varepsilon + \frac{1}{2}\tau\frac{d}{d\tau}\varepsilon. \tag{1}$$

It is quite convenient to eliminate explicit dependence on the number of colors N_c and degrees of freedom by introducing an *effective* temperature $T_{\rm eff}$ through

$$\langle T_{\tau\tau}\rangle \equiv \varepsilon(\tau) \equiv N_c^2\frac{3}{8}\pi^2 T_{\rm eff}^4. \tag{2}$$

Let us emphasize that $T_{\rm eff}$ does not imply in any way thermalization. It just measures the temperature of a thermal system with an identical energy density as $\varepsilon(\tau)$.

All-order viscous hydrodynamics amounts to presenting the energy-momentum tensor as a series of terms expressed in terms of flow velocities u^μ and their derivatives with coefficients being proportional to appropriate powers of $T_{\rm eff}$, the proportionality constants being the transport coefficients. For the case of $\mathcal{N} = 4$ plasma, the above mentioned form of $T_{\mu\nu}$ is not an assumption but a result of a derivation from AdS/CFT [7]. Hydrodynamic equations are just the conservation equations $\partial_\mu T^{\mu\nu} = 0$, which are by construction *first-order* differential equations for $T_{\rm eff}$.

In the case of boost-invariant conformal plasma, this leads to a universal form of first-order dynamical equations for the scale invariant quantity $w = T_{\rm eff}\tau$, namely,

$$\frac{\tau}{w}\frac{d}{d\tau}w = \frac{F_{\rm hydro}(w)}{w}, \tag{3}$$

where $F_{\rm hydro}(w)$ is completely determined in terms of the transport coefficients of the theory, much in the spirit of [12]. For $\mathcal{N} = 4$ plasma at strong coupling, $F_{\rm hydro}(w)/w$ is known explicitly up to terms corresponding to 3rd order hydrodynamics [13]

$$\frac{2}{3} + \frac{1}{9\pi w} + \frac{1-\log 2}{27\pi^2 w^2} + \frac{15 - 2\pi^2 - 45\log 2 + 24\log^2 2}{972\pi^3 w^3} + \ldots. \tag{4}$$

The importance of formula (3) lies in the fact that *if* the plasma dynamics would be governed entirely by (even resummed) hydrodynamics including dissipative terms of arbitrarily high degree, then on a plot of $\frac{\tau}{w}\frac{d}{d\tau}w \equiv F(w)/w$ as a function of w trajectories for all initial conditions would lie on a *single* curve given by $F_{\rm hydro}(w)/w$. If, on the other hand, genuine nonequilibrium processes would intervene, we would observe a wide range of curves which would merge for sufficiently large w when thermalization and transition to hydrodynamics would occur.

In Fig. 1(a) we present this plot for 29 trajectories corresponding to different initial states. It is clear from the plot that nonhydrodynamic modes are very important in the initial stage of plasma evolution, yet for all the sets of initial data, for $w > 0.7$ the curves merge into a single curve characteristic of hydrodynamics. In Fig. 1(b) we show a plot of pressure anisotropy $1 - \frac{3p_L}{\varepsilon} \equiv 12\frac{F(w)}{w} - 8$ for a selected profile and compare this with the corresponding curves for 1st, 2nd, and 3rd order hydrodynamics. We observe, on the one hand, a perfect agreement with hydrodynamics for $w > 0.63$ and, on the other hand, a quite sizable pressure anisotropy in that regime, which is nevertheless completely explained by dissipative hydrodynamics (see [10] for similar conclusion).

In order to study the transition to hydrodynamics in more detail, we will adopt a numerical criterion for thermalization which is the deviation of $\tau\frac{d}{d\tau}w$ from the 3rd order hydro expression (4)

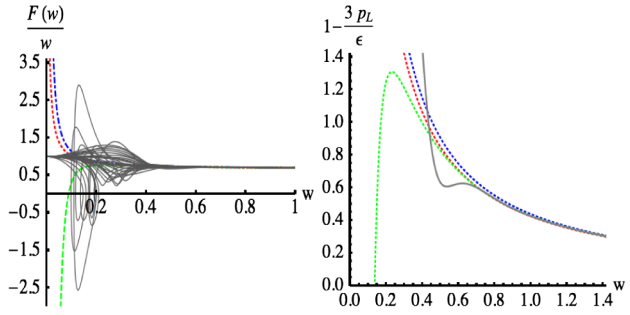

FIG. 1 (color online). (a) $F(w)/w$ versus w for all 29 initial data. (b) Pressure anisotropy $1 - \frac{3p_L}{\varepsilon}$ for a selected profile. Dashed lines (from above) represent 2nd, 1st, and 3rd order hydrodynamic fits, respectively.

$$\left| \frac{\tau \frac{d}{d\tau} w}{F^{3^{rd}\text{order}}_{\text{hydro}}(w)} - 1 \right| < 0.005. \quad (5)$$

Despite the bewildering variety of the nonequilibrium evolution, we will show below that there exist, however, some surprising regularities in the dynamics.

Initial and final entropy.—Apart from the energy-momentum tensor components, a very important physical property of the evolving plasma system is its entropy density s [per transverse area and unit (spacetime) rapidity]. In the general time-dependent case, the precise holographic dictionary for determining entropy is missing. Nevertheless, in the present case, due to high symmetry, entropy seems to be defined unambiguously in terms of $1/4G_N$ of the apparent horizon (AH) area element mapped onto the boundary along ingoing radial null geodesics [10,14,15].

For all of the initial profiles that we considered, we observed an apparent horizon that was pierced by a radial null geodesic starting from $\tau = 0$ on the boundary (see Fig. 2). This shows that the initial conditions always had some entropy per unit rapidity to start with.

The main very surprising observation of our work is that the initial entropy density measured in units of effective temperature at $\tau = 0$ is a key characterization of the initial state which, to a large extent, determines the features of the subsequent transition to hydrodynamics as well as the final produced entropy.

In the following it is convenient to introduce a dimensionless entropy density $s_{n\text{-eq}} = s_{\text{AH}}/[\frac{1}{2}N_c^2\pi^2(T^{(i)}_{\text{eff}})^2]$. In order to evaluate the final entropy density at $\tau = \infty$, we adopted the following strategy. After observing a passage to hydrodynamics, we fitted a 3rd order hydrodynamic expression for T_{eff},

$$T_{\text{eff}} = \frac{\Lambda}{(\Lambda\tau)^{1/3}}\left[1 - \frac{1}{6\pi(\Lambda\tau)^{2/3}} + \frac{-1 + \log 2}{36\pi^2(\Lambda\tau)^{4/3}} + \frac{-21 + 2\pi^2 + 51\log 2 - 24\log^2 2}{1944\pi^3(\Lambda\tau)^2}\right] \quad (6)$$

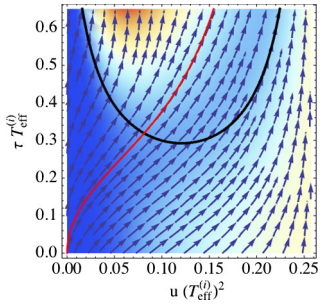

FIG. 2 (color online). The apparent horizon (black U-shaped curve) and a radial null geodesic (red curve) sent from the boundary (left edge of the plot) at $\tau = 0$ into the bulk for a sample profile. u is a bulk coordinate.

to obtain the remaining single scale Λ. Since at $\tau = \infty$ perfect fluid hydrodynamics applies, we can use the standard expression for entropy to get $s^{(i)}_{n\text{-eq}} = \Lambda^2(T^{(i)}_{\text{eff}})^{-2}$.

Once this has been done we can now determine the entropy production $s^{(f)}_{n\text{-eq}} - s^{(i)}_{n\text{-eq}}$ as a function of $s^{(i)}_{n\text{-eq}}$ for all the considered profiles. Despite the huge differences in the evolution evident in Fig. 1(a), we observe a clear functional dependence of the entropy production on the initial entropy. The results are shown in Fig. 3 together with a fit $s^{(f)}_{n\text{-eq}} - s^{(i)}_{n\text{-eq}} = 1.64(s^{(i)}_{n\text{-eq}})^{1.58}$.

Properties of thermalization.—We will now proceed to study in detail the properties of the transition from far-from-equilibrium regime to hydrodynamics. We will adopt the criterion (5), which imposes quite precise agreement between the equations of motion coming from third order hydrodynamics (being the most precise description currently known) and the actual evolution of the energy density of the plasma obtained from numerically solving the full Einstein's equations. This criterion is quite different from criterions based on isotropization of the longitudinal and transverse pressures like the one adopted in [8]. In particular, Fig. 1(b) shows quite a sizable pressure anisotropy, which is nevertheless entirely due to hydrodynamic modes.

Using the criterion (5), we determine the thermalization times for 29 initial profiles. If we were to modify the threshold, the thermalization time would of course shift, but for most profiles not significantly [11]. However, it is fair to say that thermalization is not a clear-cut event but rather happens in some narrow range of proper times.

With this proviso we will now proceed to analyze the following features of the thermalization time: (i) the dimensionless parameter $w = T_{\text{eff}}\tau$, (ii) the thermalization time in units of initial temperature, and (iii) the ratio of the effective temperature at the time of thermalization to the initial (effective) temperature.

In Fig. 4, we show a plot of the values of w at the time of thermalization as a function of the initial entropy. We see that for a wide range of initial entropies, the values of w at thermalization are approximately constant and decrease only for initial data with very small entropies.

Subsequently, we found an unexpectedly strong correlation of the thermalization time with the initial entropy

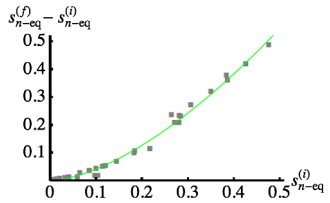

FIG. 3 (color online). Entropy production as a function of initial entropy.

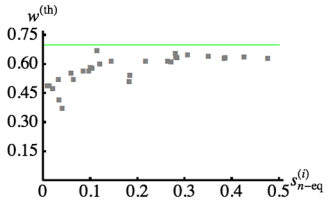

FIG. 4 (color online). The dimensionless parameter $w = \tau T_{\mathrm{eff}}$ at thermalization as a function of the initial entropy $s^{(i)}_{n\text{-eq}}$. The straight line corresponds to $w^{(\mathrm{th})} = 0.7$.

(see Fig. 5). This is very surprising, taking into account the huge qualitative differences in the evolution of the plasma when starting from various initial conditions.

Another important aspect is the question of which part of the cooling process of the plasma occurs in the far-from-equilibrium regime, and which part occurs within hydrodynamic evolution. This can be quantified by the ratio of the effective temperatures at the thermalization time and at $\tau = 0$. The plot in Fig. 5 shows a very clear correlation of this quantity with the initial entropy. The meaning of the points with high entropy requires some comment. We found that for these initial conditions, the energy density initially rises and only later decreases; thus, even a ratio of $T^{(\mathrm{th})}_{\mathrm{eff}}/T^{(i)}_{\mathrm{eff}}$ close to 1 is realized after a sizable nonequilibrium evolution [11].

Conclusions.—The crucial new feature of the holographic studies of Bjorken flow reported here is the ability to track physical observables from the far-from-equilibrium regime at $\tau = 0$ up to thermalization and subsequent hydrodynamic evolution without introducing any deformations in the field theory Lagrangian. The initial state is highly anisotropic and , in particular, always has a negative longitudinal pressure [8,9]. Despite the very rich early time dynamics, which, depending on the initial state, might have a plateau, a bump, or a sharp decrease in the effective temperature as a function of proper time, we uncovered surprising regularities in the behavior of the total produced entropy and effective temperature at thermalization as functions of initial entropy (all measured in units of effective temperature at $\tau = 0$). An interesting curiosity is that despite describing an expanding medium,

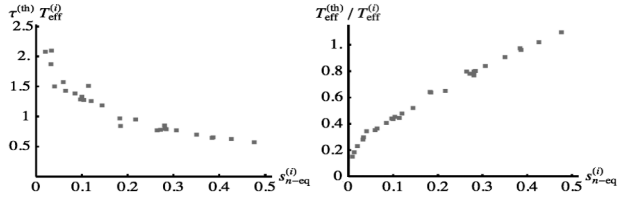

FIG. 5. The thermalization time in the units of initial effective temperature (left) and the ratio of thermalization and initial effective temperatures $T^{(\mathrm{th})}_{\mathrm{eff}}/T^{(i)}_{\mathrm{eff}}$ (right) as functions of the initial entropy $s^{(i)}_{n\text{-eq}}$.

the effective temperature at thermalization might be higher than the initial one for initial states with sufficiently big entropy. For initial states with small entropy, the energy density at thermalization is much smaller than the one at $\tau = 0$, and hence a significant part of the cooling process is of a nonequillibrium nature. Moreover, we observe generically a sizable pressure anisotropy at thermalization, which is nevertheless entirely understood in terms of dissipative hydrodynamics. An effective thermalization time $w^{(\mathrm{th})} = T^{(\mathrm{th})}_{\mathrm{eff}}\tau^{(\mathrm{th})}$, i.e., thermalization time measured in units of the effective temperature at thermalization depends on the initial state, but not strongly, and is between 0.37 and 0.67 for all considered initial states (a reasonable RHIC estimate, $T = 500$ MeV and $\tau = 0.25$ fm$/c$ gives $w = 0.63$). Finally, let us note that we could associate with all these initial data, an initial entropy already at $\tau = 0$ due to the presence of an apparent horizon. This observation shows that the thermalization and applicability of (all-order) viscous hydrodynamics is not necessarily associated with the sudden appearance of a horizon.

We thank A. Rostworowski for collaboration during the initial stages of the project, W. Florkowski, J.-Y. Ollitrault and T. Romańczukiewicz for answering many questions. This work was supported by Polish science funds as research projects N N202 105136 (2009-2012) and N N202 173539 (2010-2012), the Foundation for Polish Science and the Foundation for Fundamental Research on Matter (FOM), part of the Netherlands Organization for Scientific Research (NWO).

*On leave from National Centre for Nuclear Research, Hoża 69, 00-681 Warsaw, Poland.
m.p.heller@uva.nl
†romuald@th.if.uj.edu.pl
‡bofh@th.if.uj.edu.pl

[1] U. W. Heinz, AIP Conf. Proc. **739**, 163 (2004).
[2] J. D. Bjorken, Phys. Rev. D **27**, 140 (1983).
[3] J. M. Maldacena, Adv. Theor. Math. Phys. **2**, 231 (1998); Int. J. Theor. Phys. **38**, 1113 (1999).
[4] R. A. Janik and R. B. Peschanski, Phys. Rev. D **73**, 045013 (2006).
[5] R. A. Janik, Phys. Rev. Lett. **98**, 022302 (2007).
[6] G. Policastro, D. T. Son and A. O. Starinets, Phys. Rev. Lett. **87**, 081601 (2001).
[7] S. Bhattacharyya, V. E. Hubeny, S. Minwalla, and M. Rangamani, J. High Energy Phys. 02 (2008) 045.
[8] G. Beuf, M. P. Heller, R. A. Janik and R. Peschanski, J. High Energy Phys. 10 (2009) 043.
[9] Y. V. Kovchegov and A. Taliotis, Phys. Rev. C **76**, 014905 (2007).
[10] P. M. Chesler and L. G. Yaffe, Phys. Rev. D **82**, 026006 (2010).

[11] M. P. Heller, R. A. Janik, and P. Witaszczyk, arXiv:1203.0755 [Phys. Rev. D (to be published)].
[12] M. Lublinsky and E. Shuryak, Phys. Rev. C **76**, 021901 (2007).
[13] I. Booth, M. P. Heller, and M. Spalinski, Phys. Rev. D **80**, 126013 (2009).
[14] S. Bhattacharyya, V. E Hubeny, R. Loganayagam, G. Mandal, S. Minwalla, T. Morita, M. Rangamani and H. S. Reall, J. High Energy Phys. 06 (2008) 055.
[15] P. Figueras, V. E. Hubeny, M. Rangamani, and S. F. Ross, J. High Energy Phys. 04 (2009) 137.